MIT Libraries | DSpace@MIT

MIT Open Access Articles

Electrospun Polyaniline Fibers as Highly Sensitive Room Temperature Chemiresistive Sensors for Ammonia and Nitrogen Dioxide Gases

Massachusetts Institute of Technology

Electrospun Polyaniline Fibers as Highly Sensitive Room Temperature Chemiresistive Sensors for Ammonia and Nitrogen Dioxide Gases

Yuxi Zhang[1][3]*, Jae Jin Kim*[2]*, Di Chen*[2]*, Harry L. Tuller*[2]*, Gregory C. Rutledge*[1]*

[1] Department of Chemical Engineering, Massachusetts Institute of Technology, 77 Massachusetts Avenue, Cambridge, MA 02139

[2] Department of Materials Science and Engineering, Massachusetts Institute of Technology, 77 Massachusetts Avenue, Cambridge, MA 02139

[3] Current address: Core Research and Development, Engineering and Process Sciences Division, The Dow Chemical Company, 2301 N. Brazosport Boulevard, Freeport, TX 77541

[*] Corresponding author email: rutledge@mit.edu

Keywords

nanofibers, electrospinning, polyaniline, gas sensors

Abstract

Electrospun polyaniline (PAni) fibers doped with different levels of (+)-camphor-10-sulfonic acid (HCSA) have been fabricated and evaluated as chemiresistive gas sensors. The experimental results, based on both sensitivity and response time, show that doped PAni fibers are excellent ammonia sensors and that undoped PAni fibers are excellent nitrogen dioxide sensors. The fibers exhibit changes in measured resistances up to sixty-fold for ammonia sensing, and more than five orders of magnitude for nitrogen dioxide sensing, with characteristic response times on the order of one minute in both cases. A time-dependent reaction-diffusion model is used to extract physical parameters from fitting experimental sensor data. The model is then used to illustrate the selection of optimal material design parameters for gas sensing by nanofibers.

1.   Introduction

Several recent studies have reported the development of different types of gas sensors in which nanofibers or nanowires are used to detect trace amounts of harmful gases effectively and rapidly. [1-6] In particular, electrically conductive polymer nanofibers have been suggested to be promising candidates as chemiresistive sensor materials.[7-9] The unique combination of high specific surface area, mechanical flexibility, room temperature operation, low cost of fabrication, and large range of conductivity change makes these materials particularly attractive as nanoscale resistance-based sensors.

Electrospinning is a convenient method to produce such polymer nanofibers, with diameters on the order of tens of nanometers to microns.[10] The resulting nonwoven fiber mats have high specific surface areas, around 1 to 100 m^2/g, compared to films and conventional fibers. Polyaniline (PAni) doped with (+)-camphor-10-sulfonic acid (HCSA) represents one of the most studied classes of electrically conductive polymers,[11] and is particularly suited to the application of gas sensing because of the ease with which its conductivity is modified. The activity of the dopant can be switched reversibly between oxidation and reduction states simply by exposure to acidic and basic gases, respectively. However, PAni is relatively hard to process into fibers, compared to most other polymers, due to its rigid backbone and relatively low molecular weight, which leads to solutions with only modest elasticity. The elastic component of the viscoelastic solution behavior has been shown to be crucial to the formation of uniform fibers in electrospinning.[12] To overcome this challenge, we have recently reported the successful production of continuous fibers of pure PAni doped with HCSA by coaxial electrospinning and subsequent removal of the shell polymer (poly(methyl methacrylate),

2

PMMA). [13] These fibers were shown to exhibit electrical conductivities as high as 130 S/cm when fully doped, and thus present a broader range of tunable conductivity with which to work during gas sensing than most of the similar systems reported to date.[14]

In this work, these electrospun PAni fibers are shown to perform effectively as nanoscale sensors for both ammonia (NH_3) and nitrogen dioxide (NO_2) gases. They are found to exhibit high sensitivities and fast response times. A reaction-diffusion model is used to characterize the reaction kinetics and molecular diffusivities of the gases within the fibers, and to design future materials for optimal sensing performance under various conditions of fiber size, gas concentration, reaction kinetics, and gas adsorption into fibers.

2. Experimental

2.1 Material

Polyaniline (PAni, emeraldine base, M_w = 65,000) was purchased from Sigma-Aldrich, Inc. The dopant, (+)-camphor-10-sulfonic acid (HCSA), was obtained from Fluka Analytical Chemicals. Poly(methyl methacrylate) (PMMA, M_w = 960,000 g/mol) was purchased from Scientific Polymer Products Inc. The N,N-dimethylformamide (DMF) and isopropyl alcohol (IPA) used were OmniSolv® solvents from EMD Chemicals. Chloroform was purchased from Mallinckrodt Chemical Inc.   Certified pre-mixed gases (1000 ppm NH_3 in dry nitrogen, 100 ppm NO_2 in dry air, dry nitrogen and dry air) were all purchased from Airgas, Inc. All materials were used without further purification.

2.2 Sample Preparation: Electrospinning

Core-shell fibers were prepared by the method of coaxial electrospinning,[15, 16] followed by selective removal of the shell as described previously.[13] The core fluid was 2 wt% PAni, blended with various amounts of HCSA, dissolved in a 5:1 mixture by weight of chloroform and DMF; the shell fluid was 15 wt% PMMA in DMF. The core and shell fluid flow rates were 0.010 mL/min and 0.050 mL/min, controlled independently by two syringe pumps. The applied voltage was 34 kV, and the distance between the spinneret and collection plate was 30 cm. After the fibers were formed, the resultant fibers and mats were then immersed in IPA for one hour with gentle stirring, so that the PMMA shell component was removed, leaving intact the doped PAni fiber cores. X-ray photoelectron spectroscopy (XPS) and differential scanning calorimetry

(DSC) were used to confirm the removal of the PMMA shell. The core-shell fibers were also post-processed to stretch the fibers longitudinally as described previously,[13] where it was shown that the molecular orientation of the PAni molecules increased with increasing longitudinal strain in the resultant fibers.

2.3 Fiber Electrical Conductivity

Fibers were electrospun onto interdigitated Pt electrodes (IDE, ABTech) with 50 sets of interdigitated fingers, and finger width and spacing ranging from 5 to 20 μm. Their electrical properties were measured with an impedance analyzer (Solartron 1260/1287A), with resistance values extracted from the frequency-dependent Nyquist plots. The measurements were performed in controlled environments at room temperature and 20% relative humidity. The fiber electrical conductivity (σ_f), with correction for contact resistance R_{f0}, was calculated according to Equation 1

$$\sigma_f = \frac{4\delta}{\pi d^2 \left(R_f - R_{f0} \right)} \tag{1}$$

where the single-fiber resistance, $R_f = (RN)$, R is the resistance measured on the IDE, N is the number of parallel pathways formed by fibers on the IDE bridging over the interdigitated fingers as observed by optical microscopy, d is the average fiber diameter obtained by scanning electron microscopy (SEM) on the as-spun fibers, and δ is the finger spacing (inter-electrode distance) of the IDE. Further details may be found in an earlier publication.[13]

2.4 Gas Sensing

Gas sensing tests were conducted in a quartz tube placed inside a Lindberg Blue TF 55035A furnace as described elsewhere,[17] and exposure of the samples to different gases was achieved using mass flow controllers (MKS Instuments) on separate streams of test gases and inert background gases. The temperature of the tube furnace remained at room temperature (20°C) and was not adjusted. The experiments were conducted inside the furnace to avoid any spurious changes in charge carrier concentrations due to external illumination. The setup is illustrated in **Figure 1**.
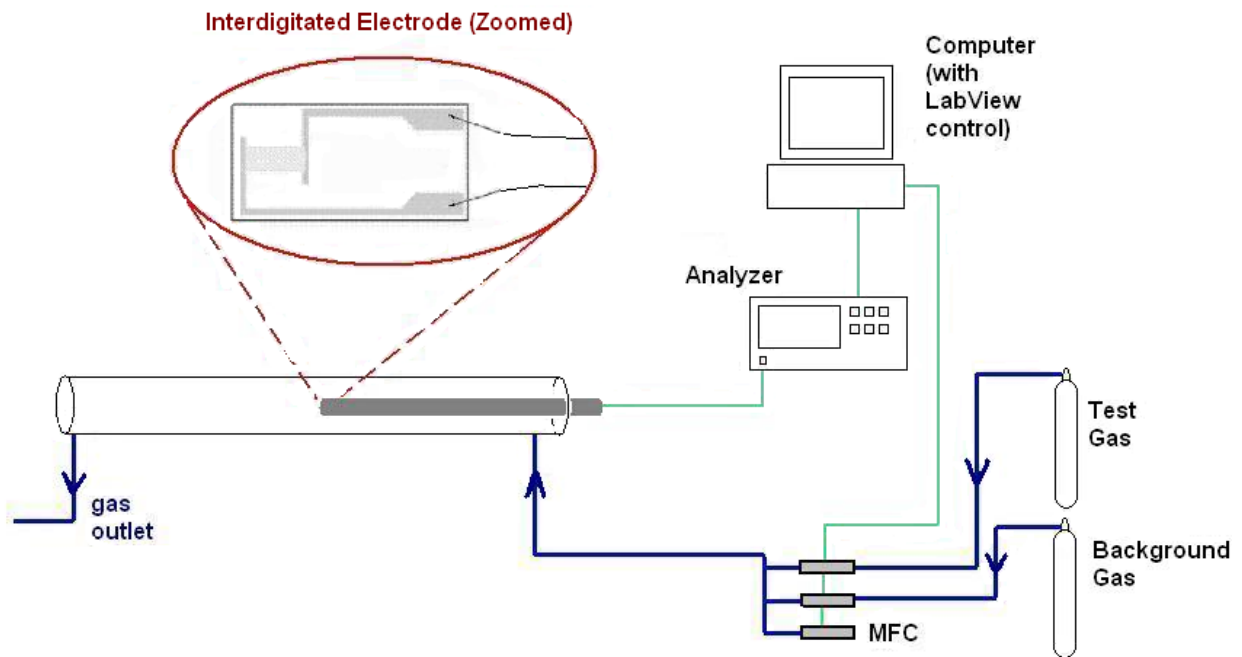

Figure 1 Illustration of gas sensing apparatus, including the tube furnace, the location of the interdigitated electrodes (IDE) (zoomed in), the mass flow controllers (MFC), the computer for LabView control and data collection and analyzer interface

All experiments were conducted with a constant total gas flow rate of 200 sccm. For NH$_3$ sensing, a certified premixed gas containing 1000 ppm of NH$_3$ in dry nitrogen was diluted with additional dry nitrogen gas by MFC's to a concentration in the range of 10 to 700 ppm of NH$_3$; for NO$_2$ sensing, a certified premixed gas containing 100 ppm of NO$_2$ in dry air was diluted with additional dry air to a concentration in the range of 1 to 50 ppm of NO$_2$. For each sample, about 10 aligned electrospun fibers were deposited on an IDE with 10 μm finger spacings. The contacts from the interdigitated electrodes to the testing apparatus were made by platinum wires. The DC resistances between the measurement portals in the quartz tube were measured by an Agilent HP34970A data acquisition system controlled by a LabView program and interface.

PAni doped with HCSA exhibits p-type semiconductor characteristics, so exposure to electron-donating species such as NH$_3$ gives rise to a decrease in the charge-carrier concentrations and thus an increase in the measured resistance. For NH$_3$ sensing, changes in resistance of doped PAni fibers are therefore reported as $\Delta R/R_0$, where $\Delta R=R_{ex}-R_0$, R_0 is the measured initial resistance prior to any exposure to NH$_3$, and R_{ex} is the measured resistance upon exposure. In contrast to NH$_3$, NO$_2$ is electron-withdrawing and thus acts as dopant in lieu of HCSA to increase the charge carrier concentration of p-type PAni. Consequently, upon exposure to NO$_2$ the measured resistance of an undoped PAni sample decreases. For NO$_2$ sensing, changes in resistance are therefore reported as $-\Delta R/R_{ex}$. The sensitivity of the materials for gas sensing, in units of ppm^{-1}, is defined as the ratio between $\Delta R/R_0$ (for ammonia) or $-\Delta R/R_{ex}$ (for nitrogen dioxide) and the concentration of the test gas in ppm, in the range of low test gas concentration where there is a linear relation between these two quantities.

2.5   QCM Analysis

A quartz crystal microbalance with dissipation monitoring (QCM-D, Q-sense)[18,19] was used to measure the change in mass of electrospun fibers due to absorption of NH_3 during exposure to a gas of fixed NH_3 concentration. A thin layer of as-electrospun PAni fibers (about 10 μm in thickness) was deposited on the quartz crystal resonator with gold electrodes. The coated resonator was placed in the Q-sense flow cell with a blank crystal as a reference. A mixture of NH_3 and nitrogen gas was introduced to the flow cell through a flow controller. Changes in both frequency and dissipation for the crystal harmonics were then recorded, and equilibrium values were obtained after 10 minutes of equilibration. The change in mass was calculated using the Saurbrey relationship

$$\Delta m = -C \frac{1}{n} \Delta f \qquad (2)$$

where Δm is the change in mass, C is a constant dependent on the crystal and $C = 17.7$ ng s cm^{-2} in this case, n is the harmonic overtone, and Δf is the frequency change.[20] For calculations, the third, fifth, and seventh harmonics ($n = 3, 5,$ and 7) were used to obtain an averaged value for the changes in mass.

3.   Results and Discussions

3.1   Morphologies and electrical properties of as-electrospun fibers

Figure 2 shows representative images of the PAni/HCSA fibers after coaxial electrospinning and removal of the PMMA shell component by dissolution in IPA. The fibers are confirmed to be smooth, relatively uniform in diameter and continuous. No significant difference in fiber diameters is observed for fibers prepared with molar ratios of HCSA to PAni of 0, 0.25, 0.50, 0.75 or 1. However, the electrical conductivities of the fibers increase exponentially with increasing molar ratio of HCSA to PAni, as shown in **Table 1**. This trend is consistent with the observations of Trchova et. al. for PAni pellets with different doping levels.[21]
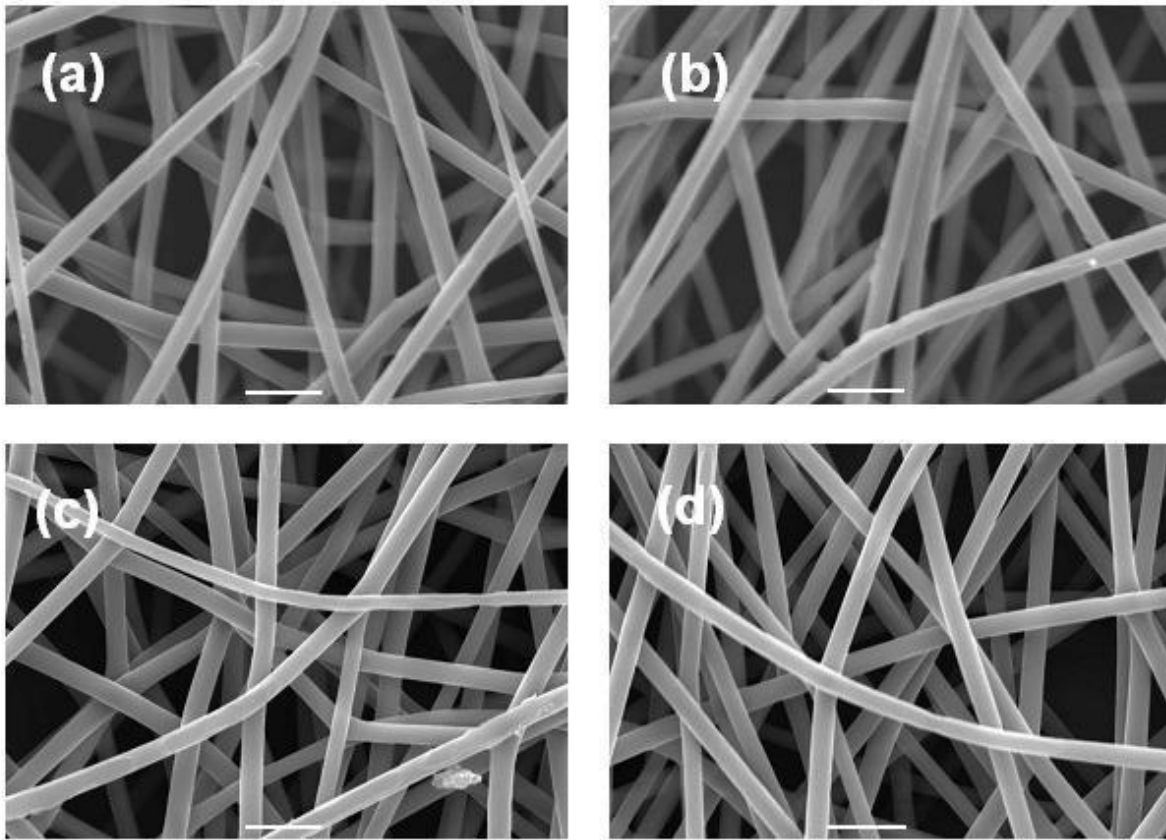
Figure 2 SEM images of electrospun PAni/HCSA fibers with different molar ratios of HCSA to PAni: [HCSA]/[PAni] = 0 (a); 0.5 (b); 0.75 (c); and 1.0 (d). All images taken after dissolution of PMMA shell and using 7,500× magnification (scale bar = 2 μm)

Table 1 Diameter and Conductivity of As-spun PAni/HCSA Fibers after Removing Shell

[HCSA]/[PAni] Mole Ratio	Diameter, d (nm)	Electrical Conductivity, σ_f (S/cm)
0	650 ± 110	$(2.0 \pm 0.6) \times 10^{-6}$
0.25	670 ± 120	0.0022 ± 0.0008
0.50	600 ± 90	0.18 ± 0.05
0.75	650 ± 110	2.3 ± 0.9
1.0	620 ± 160	50 ± 30

3.2 Ammonia Sensing

The PAni fibers with HCSA:PAni mole ratio of 1 were used for sensing experiments with NH_3 for concentrations from 10 to 700 ppm. Both as-electrospun fibers (average fiber diameter = 620 nm) and after solid-state drawing (average fiber diameter = 450 nm) were tested.

The gas sensing responses are fast, as demonstrated by a representative plot of $\Delta R/R_0$ versus time for drawn PAni fibers with diameter of 450 nm shown in **Figure 3**. The PAni fibers were exposed to repeated cycles of 5 min exposure to a gas stream of 500 ppm of ammonia (balance nitrogen) followed by 5 min of nitrogen purging. The response time is defined as the time required for the change in signal to reach within $1/e$ of the total difference between steady state values obtained during exposure and purging. For the case shown in Figure 3, the average response time is 45 ± 3 seconds upon exposure, and 63 ± 9 seconds for recovery upon purging.

11

The results also show that the measurement was reasonably reversible; the maximum $\Delta R/R_0$ value did not vary much over multiple cycles of exposure to the same concentration of gases, so that the fibers can be used multiple times for sensing. However, there was an increase of baseline resistance after the first cycle in some cases, as seen in the case shown in Figure 3, indicating that nitrogen purging alone is not enough to return the fibers to the original state, i.e., some ammonia molecules have irreversibly reacted with or bound to the fibers. The baseline does not increase after subsequent cycles, so that the sensing measurements are reversible after the first cycle of exposure in all cases.
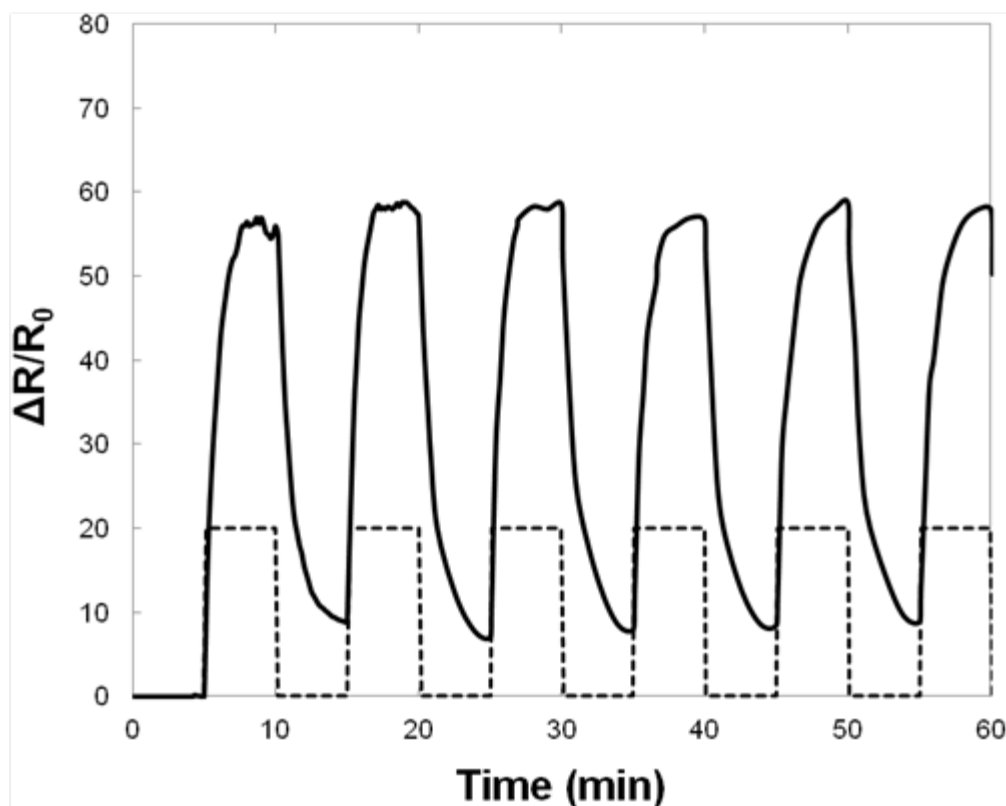

Figure 3 Time response (solid curve) of drawn PAni fiber with mole ratio [HCSA]/[PAni] = 1.0 (d = 450 nm) under cyclic exposure of 500 ppm of ammonia; dashed lines indicates the change in ammonia concentration between 0 and 500 ppm

12

Table 2 Characteristic Response Times of As-Spun and Solid-State-Drawn PAni/HCSA Fibers with Mole Ratio [HCSA]/[PAni] = 1.0 during Ammonia Exposure and Nitrogen Purge

NH$_3$ Concentration (ppm)	Response time (s) for as-spun PAni fiber		Response time (s) for solid-state drawn PAni fiber	
	Exposure	Purging	Exposure	Purging
20	84 ± 6	133 ± 8	82 ± 3	109 ± 9
50	82 ± 4	92 ± 4	67 ± 5	84 ± 4
100	66 ± 6	75 ± 2	59 ± 8	83 ± 5
500	43 ± 3	61 ± 8	45 ± 3	63 ± 9
700	31 ± 4	53 ± 6	28 ± 5	47 ± 7

PAni fibers were then subjected to longer exposures of ammonia for concentrations ranging from 10 to 700 ppm. **Table 2** lists the characteristic response times (averaged over at least three cycles) of the as-spun and solid-state drawn PAni fibers with different levels of ammonia exposure. Response times decrease monotonically with increasing ammonia concentration. The recovery times with nitrogen purging are significantly longer than the exposure responses times. When comparing the as-spun and solid-state drawn PAni fibers, the drawn fibers tend to have slightly faster response times, but the difference is not significant. The difference could be due to both the smaller fiber diameter and the high level of molecular orientation that comes with solid state drawing. In general, 10 minutes is sufficient for the signals to reach steady state during both exposure and purging, as shown in the time response of fibers to exposure of different concentration of ammonia in **Figure 4**.
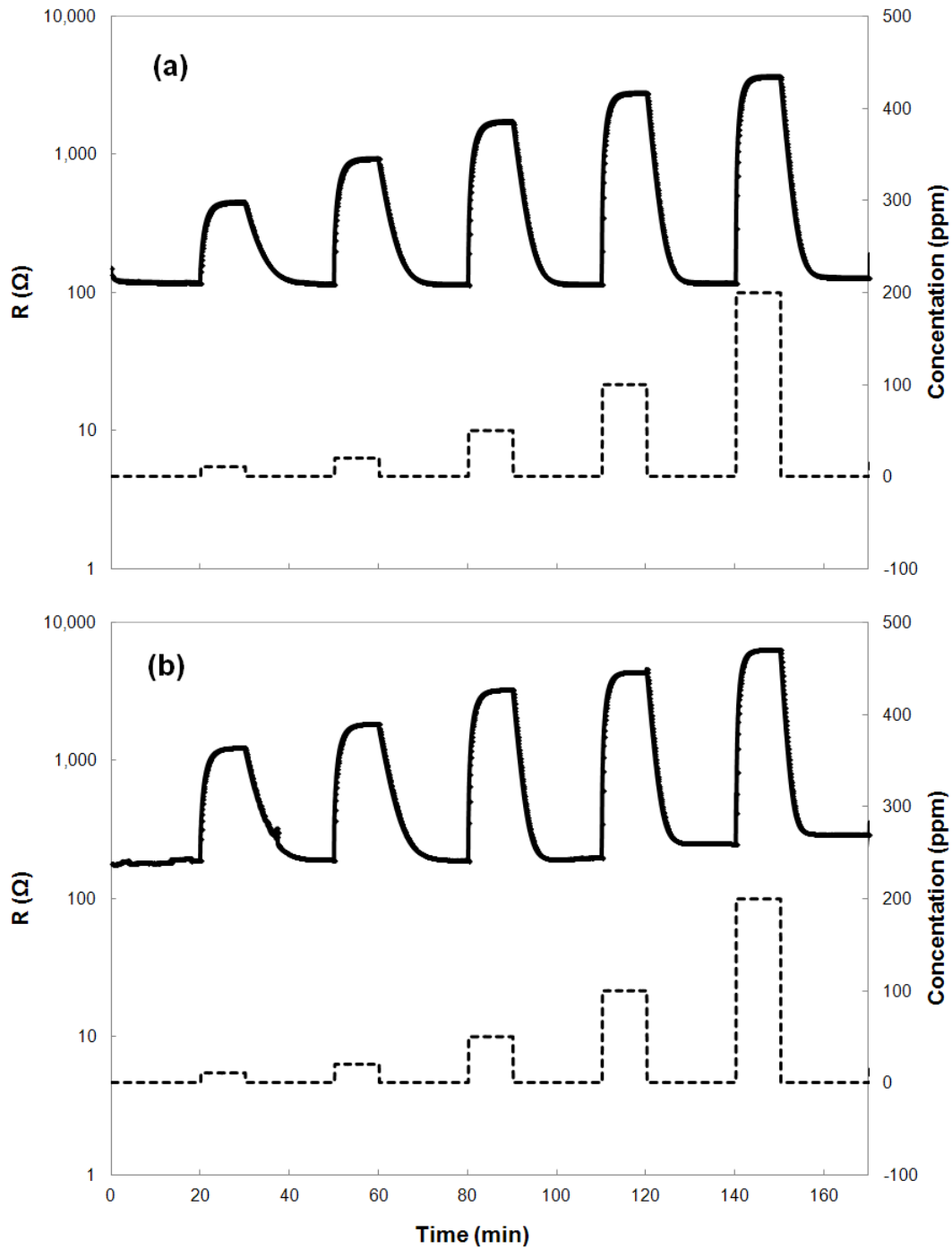
Figure 4 Time response of (a) as-spun doped PAni fibers (d = 620 nm) and (b) solid-state drawn doped PAni fibers (d = 450 nm), to different concentrations of NH_3; dashed lines show the change in NH_3 concentration in the test gas. The mole ratio of [HCSA]/[PAni] is 1.0.
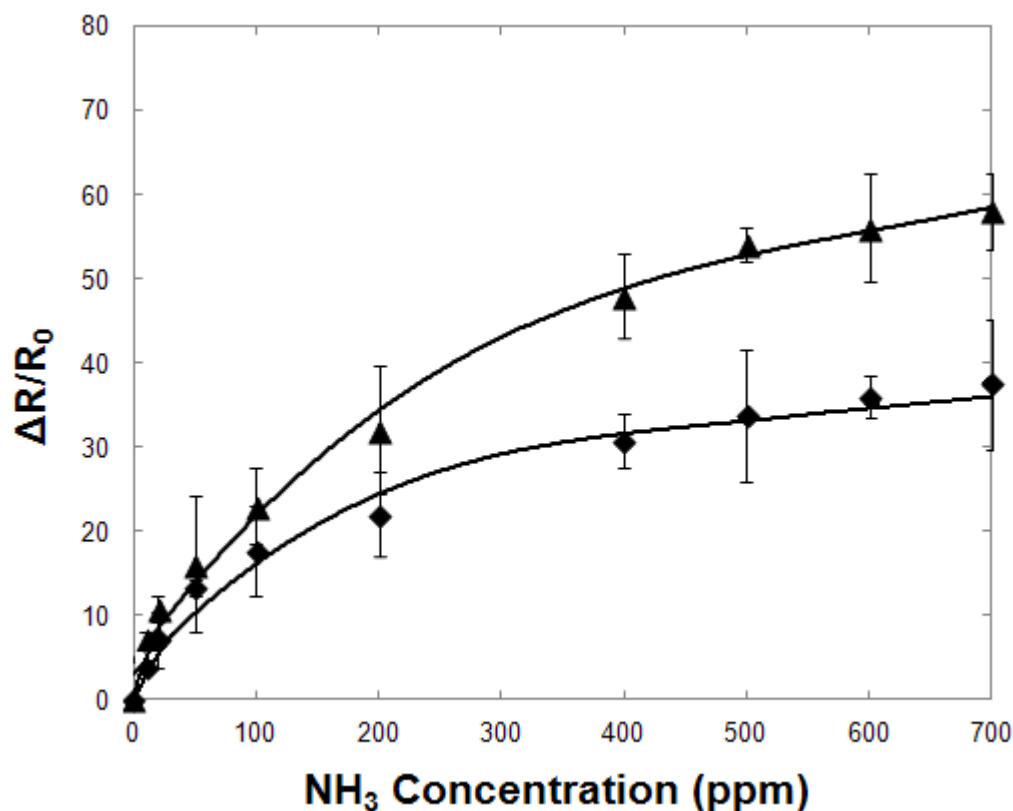
Figure 5 Changes in resistance upon exposure of electrospun PAni fibers with mole ratio [HCSA]/[PAni]=1.0 to different concentrations of ammonia gas; as-spun fibers (d = 620 nm) (filled diamonds); solid-state drawn fibers (d = 450 nm) (filled triangles); and lines with best polynomial fits to the data

The steady-state responses after 10 min exposures of ammonia are shown in **Figure 5** as a function of increasing ammonia concentration from 10 to 700 ppm. The measured resistances of both as-spun and solid-state drawn HCSA-doped PAni fibers increase dramatically upon exposure to NH_3. Responses as large as $\Delta R/R_0 = 38 \pm 8$ were observed at 700 ppm ammonia for the as-spun PAni fibers (d = 620 nm), and 58 ± 5 for the solid-state drawn PAni fibers (d = 450 nm). Such large responses are among the highest thus far reported for PAni or PAni-composite fibers, and are advantageous for gas sensing where signal-to-noise ratios can be an issue.[22] In

15

the linear region of exposure to concentrations below 20 ppm of ammonia, the sensitivity of the

620 nm fiber is 3.5 ppm^{-1}, and the sensitivity of the 450 nm fiber is 5.5 ppm^{-1}, both of which are

much higher than the sensitivity of a cast film of the same material with 10 μm thickness,

measured at 0.02 ppm^{-1}.   The ammonia exposure limit in the United States is 25 ppm over an

eight-hour period, and 35 ppm over a short-term exposure.[23]   The level of sensitivity exhibited

by these fibers is sufficient for rigorous environmental monitoring at these levels.

3.3   Nitrogen Dioxide Sensing

For NO$_2$ gas sensing, as-spun undoped PAni fibers (i.e., mole ratio [HCSA]/[PAni]= 0, d

= 650 nm) were tested. The representative time response is shown in **Figure 6** for the exposure

of undoped PAni electrospun fibers to concentrations of NO$_2$ between 1 and 50 ppm. As is in

the case of NH$_3$ sensing, the response time is defined as the time required for the signal to reach

within 1/e of the total difference between steady state values obtained during exposure and

purging. Similar to the NH$_3$ sensing system, the undoped PAni fiber sensor also shows quick

response times and good recovery. **Table 3** lists the characteristic response times of the undoped

PAni fibers to NO$_2$ exposure. The response times are on the order of 50 s for exposure and 70 s

for purging, and do not vary much within the range of concentrations from 1 to 50 ppm.
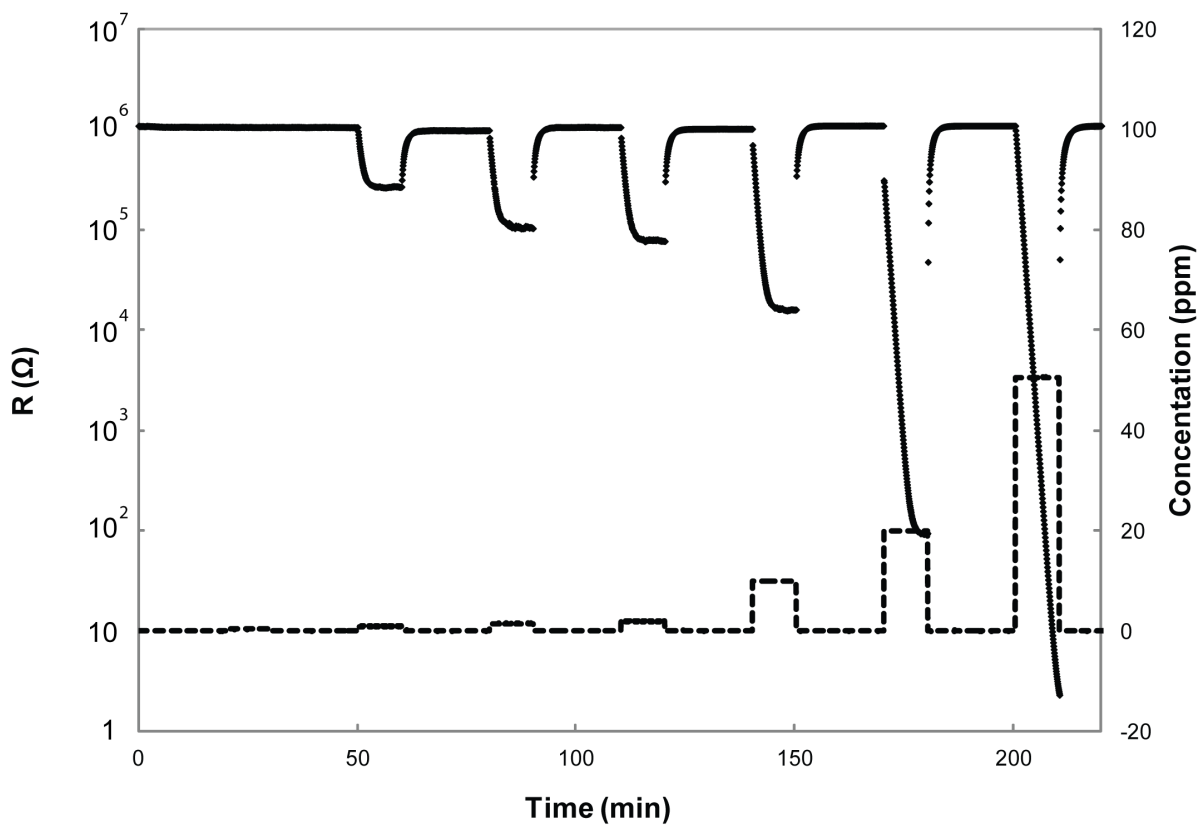
Figure 6 Time response (solid circles) of as-spun undoped PAni fibers (d = 650 nm) under cyclic exposure to increasing concentrations of NO$_2$ (dashed line)

Table 3 Characteristic Response Times of Undoped PAni Fibers during NO_2 Exposure and Purge

NO$_2$ Concentration (ppm)	Response Time (s)	
	Exposure	Purging
1	55 ± 5	68 ± 8
2	50 ± 9	71 ± 6
5	48 ± 3	62 ± 5
10	45 ± 3	61 ± 8
20	43 ± 3	67 ± 8
50	46 ± 5	82 ± 9

Figure 7 shows the response of the undoped PAni fibers to NO_2 exposure with concentrations in the range between 1 and 50 ppm. The reported $\Delta R/R_{ex}$ values are taken after 10 minutes of sustained exposure. The resistance decreases remarkably upon exposure to NO_2 concentrations between 1 and 50 ppm. The huge response, up to almost 6 orders of magnitude, indicates that pure PAni fibers can be very effective NO_2 sensors, changing PAni from its undoped, insulating state to almost the fully doped, high conductivity state. The response at 1 ppm is a more than 80% decrease in resistance, indicating very good sensitivity even under exposure to very low concentrations of NO_2. The exposure limit set by the environmental agencies in the US for NO_2 is 50 ppb,[24] which is a concentration too low to be tested directly with the gas composition and flow controllers available for this work. However, based on extrapolations at low NO_2 concentrations, it is reasonable to expect at least a 15% decrease in

resistance for these PAni fibers when exposed to 50 ppb NO_2, a response that should be easily detectable. With their large response magnitude and short response time, these PAni fibers can serve as the basis of a very effective nanoscale sensor for NO_2.
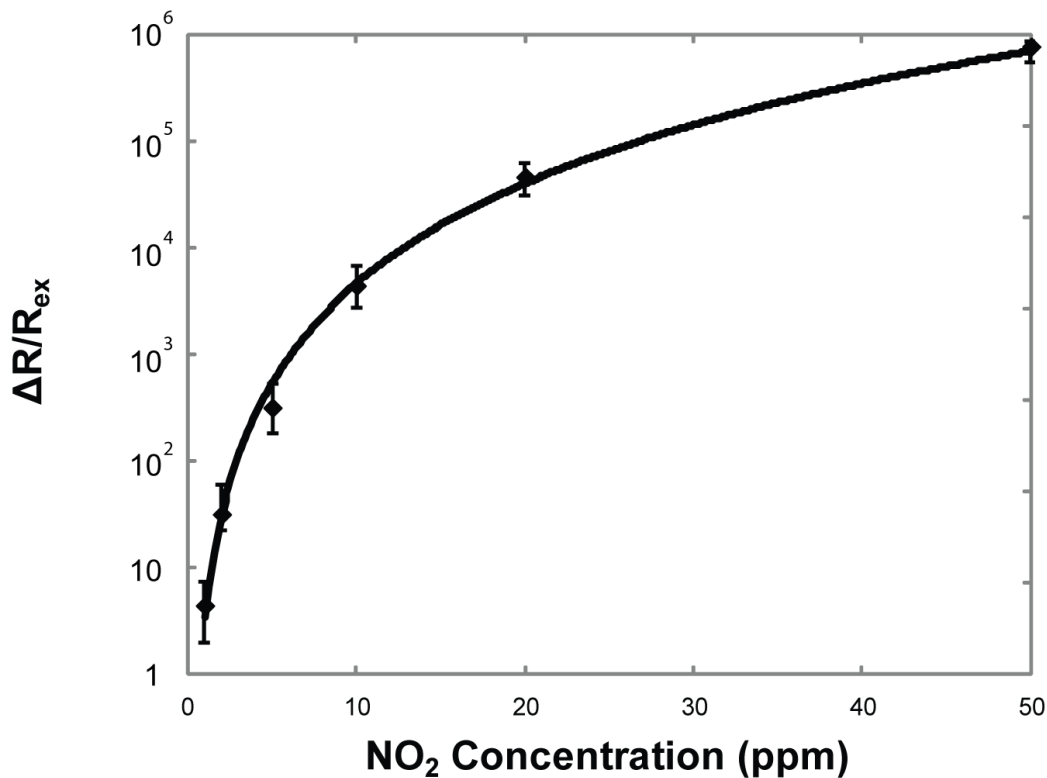

Figure 7 Changes in resistance upon exposure of as-spun undoped electrospun PAni fiber (d = 650 nm) to different concentrations of NO_2 gas

NH_3 and NO_2 gases have been chosen as examples of reducing and oxidizing gases, respectively, to show the exceptional gas sensing performance of the electrospun PAni fibers. Because of the ease with which PAni is doped or de-doped, these fibers are expected to be responsive to a variety of acidic and basic gases. However, due to differences in reaction and

adsorption equilibria, diffusivities and other factors, different gases are expected to produce different response times and magnitudes of response upon exposure. Such differences can be analyzed using the methods presented in the next section, where we model the gas sensing of these fibers. Such differences in response can then be used as a means for selectively distinguishing between different gases.

3.4   Reaction-Diffusion Model

A major difference between the experimental results for NH_3 and NO_2 sensing is that $\Delta R/R_{ex}$ for NO_2 undergoes changes in resistance of up to 6 orders of magnitude, while $\Delta R/R_0$ for NH_3 exhibits less than two orders of magnitude change. It is apparent from the values for conductivity in Table 1 that the whole range of doping levels is not being explored in the NH_3 case. The most likely explanation is that ammonia, being a relatively weak base, does not fully deprotonate the doped PAni in the presence of the acidic HCSA, even at concentrations as high as 700 ppm. This can be explained by a reaction equilibrium between the doped PAni and NH_3:

Scheme 1: $PAni\text{-}H^+ + NH_3 \rightleftarrows PAni + NH_4^+,$
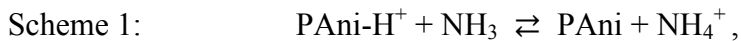
wherein the equilibrium lies somewhere in the middle rather than to either extreme, i.e.,

$$\frac{[PAni]}{[PAni-H^+]} = \frac{K[NH_3]}{[NH_4^+]} : 1 \ . \tag{3}$$

On the other hand, because the PAni fibers used for nitrogen dioxide sensing were undoped, the incoming NO_2 serves as the only available acidic dopant for PAni; there is no competing strong acid/base in the system. The huge change of conductivity suggests that the reaction is mostly irreversible, or the equilibrium lies very much to the right (K approaches ∞).

To characterize the changes in resistance observed in this work, we model the fibers as simple cylindrical elements in which gases diffuse radially into the fiber upon exposure. The model is simplified by assuming that the chemical composition (and thus conductivity) of the fibers varies only with radial position, so that the overall observed change in resistance can be expressed as

$$\frac{R_{ex}}{R_0} = \frac{\sigma_0 L^2}{2\int_0^L \sigma(\Phi(r))r\,dr} \tag{4}$$

where r is the radial position in the fiber, L is the characteristic length, which is the fiber radius in this case, σ_0 is the fiber conductivity prior to exposure, and $\sigma(\Phi(r))$ is the radially varying conductivity as a function of concentration of the reactive component in the fiber $(\Phi(r))$ and thus a function of r. This model can be thought of as concentric shells in the fiber forming parallel conducting pathways throughout the length of the fiber, with the inverse of total resistance for the fiber being the sum of the inverse resistances (conductivities) for each concentric shell weighted by its respective cross-sectional area.

A reaction-diffusion model can be used to model both the spatial and temporal changes in the electrospun fibers upon gas exposure. With the assumption that the reaction is reversible and first order with respect to each of its reactants and products, the concentration changes can be described generically by the following system of partial differential equations:

$$\frac{\partial \Theta}{\partial \tau} = \frac{1}{r} \frac{\partial}{\partial r}\left(r \frac{\partial \Theta}{\partial r} \right) + \alpha \left[-\text{Da } \Theta\Phi + \frac{\text{Da}}{K}\Omega\Psi \right] \tag{5}$$

$$\frac{\partial \Phi}{\partial \tau} = -\text{Da } \Theta\Phi + \frac{\text{Da}}{K}\Omega\Psi \tag{6}$$

$$\frac{\partial \Omega}{\partial \tau} = \alpha \left[\text{Da } \Theta\Phi - \frac{\text{Da}}{K}\Omega\Psi \right] \tag{7}$$

$$\frac{\partial \Psi}{\partial \tau} = \text{Da } \Theta\Phi - \frac{\text{Da}}{K}\Omega\Psi \tag{8}$$

Here, Θ is the normalized concentration of the diffusing gaseous reactant (e.g. NH_3 or NO_2), Φ is the normalized concentration of the non-diffusing reactant (e.g., PAni or PAni-H^+), Ψ is the normalized concentration of the polymeric product of reaction (e.g., PAni-H^+ or PAni), and Ω is the normalized concentration of the other product of reaction (e.g., NH_4^+ or NO_2^-). r is the normalized radius r/L. τ is the dimensionless time $\tau = t/t_D = tD/L^2$ with D being the diffusivity of the diffusing gaseous reactant within the fiber. Da is the Damköhler number, defined as the dimensionless number representing the ratio of the reaction time constant, with respect to the forward reaction and reference concentration of Θ, to the diffusion time constant, so that . $Da = k_f C_{0,\Theta} L^2/D$. K is the equilibrium constant of the reaction, also the ratio of the forward to

reverse reaction rate constants $K = k_f/k_r$. α is the dimensionless ratio of the reference

concentrations for the non-diffusing and diffusing reactant: $\alpha = C_{0,\alpha}/C_{0,e}$. Because of their

corresponding stoichiometric ratios, the reference concentration of Ψ, $C_{o,\Psi}$, is set equal to the

reference concentration of Φ, and the reference concentration of Ω, $C_{o,\Omega}$, is set equal to the

reference concentration of Θ. Equation 5 expresses the dynamics for the concentration of the

gaseous reactant, which include diffusion down a concentration gradient, consumption by the

forward reaction and production by the reverse reaction. Equation 7 expresses the dynamics for

the concentration of the product formed from the gaseous reactant; as the product is generally

ionic and believed to bind closely with the oppositely charged ions on the polymeric substrate,

the dynamics do not include diffusion (assumed to be negligible), but include only production by

the forward reaction and consumption by the reverse reaction. Equation 6 (or 8) expresses the

dynamics for the concentration of the polymeric reactant (product), which also include only

consumption (production) by the forward reaction and production (consumption) by the reverse

reaction.

With the specification of appropriate boundary and initial conditions, this system can be

solved numerically by MATLAB for specified values of the parameters. If one assumes that

only the non-diffusing polymeric reactant is present in the system initially, and the initial

concentrations of solute species (both reactant and product) within the fiber are zero, the

boundary and initial conditions for the cylindrical system can be described as follows:

$$\Theta(1,\tau) = 1, \quad \frac{\partial \Theta}{\partial r}(0,\tau) = 0, \quad \Theta(r,0) = 0$$

$$\Phi(r,0) = 1$$
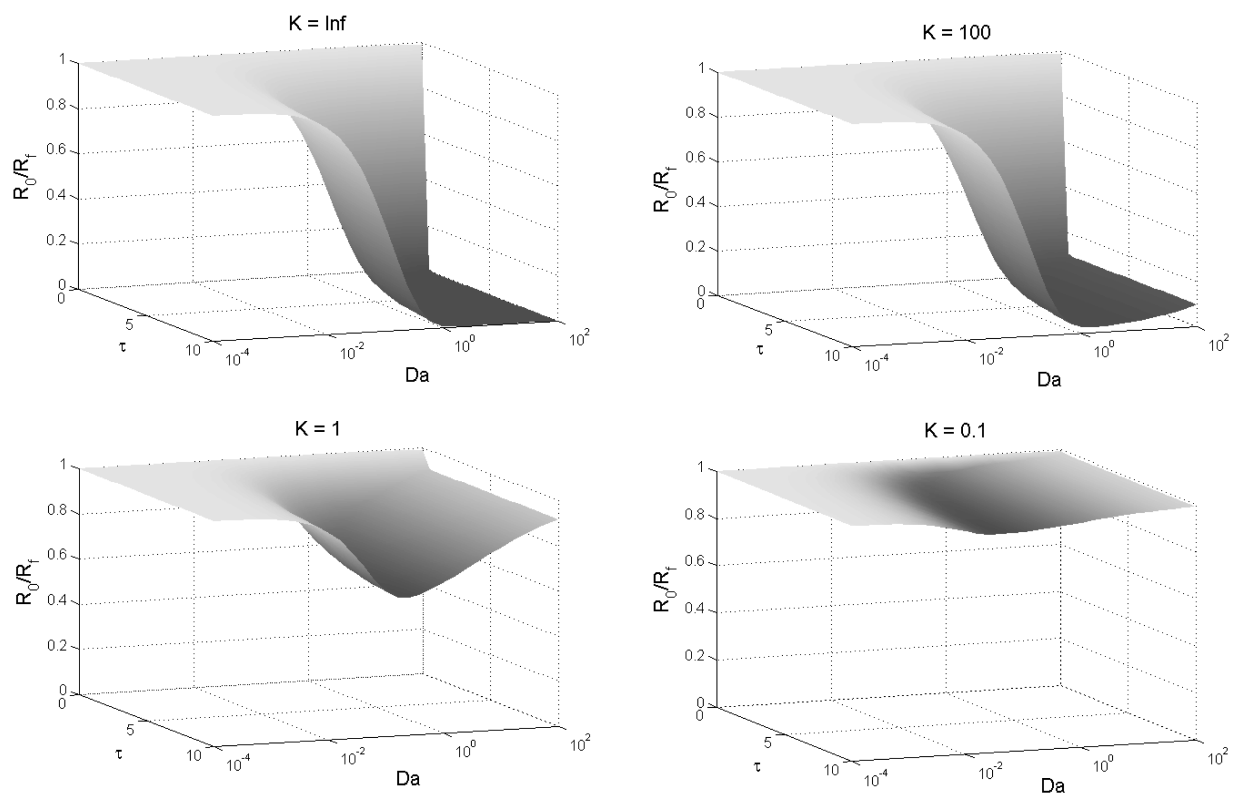
$$\Omega(r,0) = 0$$

$$\Psi(r,0) = 0$$

Figure 8 Results of reaction-diffusion model showing the ratio of resistances prior to and after exposure, plotted as a functions of Damköhler number (Da) and dimensionless time (τ) for selected values of equilibrium constant (K). Calculations assume that no gaseous reactant or product is present in the fibers as the initial condition, and that the conductivity of the fiber decreases linearly with the concentration of the reactant Φ

Figure 8 shows the results of this reaction-diffusion model, where the ratio of initial to final resistances is plotted as a function of Da and τ at selected values of K = ∞, 100, 1, and 0.1. For these calculations, we assume that the initial concentrations of small molecular solute species are zero, and that the conductivity of a section of the fiber decreases linearly with the concentration of the reactant Φ.

One can see that the resistance increases (R_0/R_{ex} decreases) monotonically with τ for all values of Da and K. If Da is very large, the reaction is much faster than the diffusion; the diffusion front is very sharp but penetrates slowly into the fibers. If Da is very small, diffusion is much faster than reaction, so that the concentration profile is almost flat within the fiber; the gas rapidly penetrates the entire fiber. However, it may still take a long time (on the dimensionless scale) for the diffused gas to react and cause the necessary change in conductivity. Significantly, there exists a minimum in R_0/R_{ex} with respect to Da at any given τ, except for the case of K = ∞ where the forward reaction is irreversible. Therefore, there exists an optimal Da value for the overall resistance of the fiber to change at the fastest rate. This suggests that systems can be optimized with respect to Da for all such reversible reactions. Recalling that $Da=k_f C_{0,s} L^2/D$, such optimization can be performed for a specific application by designing the fiber diameter for the target exposure concentration. Indirectly, Da can also be altered by changing the fiber material, gas species, or temperature, factors that all affect the reaction rate constant and diffusivity.

3.5   Fitting Model Parameters from Experimental Data

25

At steady state, where there is no longer dependence on time, the system of equations simplifies to:

$$\frac{\partial \Theta}{\partial \tau} = \frac{1}{r}\frac{\partial}{\partial r}\left(r\frac{\partial \Theta}{\partial r}\right) = 0 \tag{5'}$$

$$\frac{\partial \Phi}{\partial \tau} = -\text{Da }\Theta\Phi + \frac{\text{Da}}{K}\Omega\Psi = 0 \tag{6'}$$

$$\frac{\partial \Omega}{\partial \tau} = \alpha\left[\text{Da }\Theta\Phi - \frac{\text{Da}}{K}\Omega\Psi\right] = 0 \tag{7'}$$

$$\frac{\partial \Psi}{\partial \tau} = \text{Da }\Theta\Phi - \frac{\text{Da}}{K}\Omega\Psi = 0 \tag{8'}$$

where equations (6'), (7') and (8') all reduce to the definition of the equilibrium constant being the ratio of the four concentrations at equilibrium, and equation (5') requires that the radial dependence of concentration disappears at steady state. Since the concentrations, and thus the fiber electrical conductivity, are no longer dependent on radial position in the fiber, this leads to the simplification in equation 4 that

$$\frac{R_{ex}}{R_0} = \frac{\sigma_0}{\sigma_{ex}} \tag{4'}$$

Equation (4') can be used to re-plot the experimental data for $\Delta R/R$ vs. gas phase concentration (at steady state) as a relationship between conductivity after exposure σ_{ex} and gas phase concentration.

Take the system of ammonia sensing, for example. Once the experimental steady state data have been converted to a plot of σ_{ex} vs. gas phase ammonia concentration, a plot such as the

one given in **Figure 9**, showing the relationship between fractions of PAni doped versus the external ammonia concentration, can be constructed. Here, we have used the results for conductivity vs [HCSA]/[PAni] shown in Table 1 as a calibration to relate conductivity to fraction of PAni doped. .

By mass balance $[PAni - H^+] + [PAni] = [PAni]_0$, where the right hand side is the original concentration of PAni present in the fibers, regardless of doping levels. Using this, the fraction of doped PAni can be related to the equilibrium constant, and written as

$$\frac{[PAni - H^+]}{[PAni]_0} = \left(\frac{K[\text{NH}_3]}{[\text{NH}_4^+]} + 1\right)^{-1} = 1 - \frac{K[\text{NH}_3]}{K[\text{NH}_3] + [\text{NH}_4^+]} \tag{9}$$
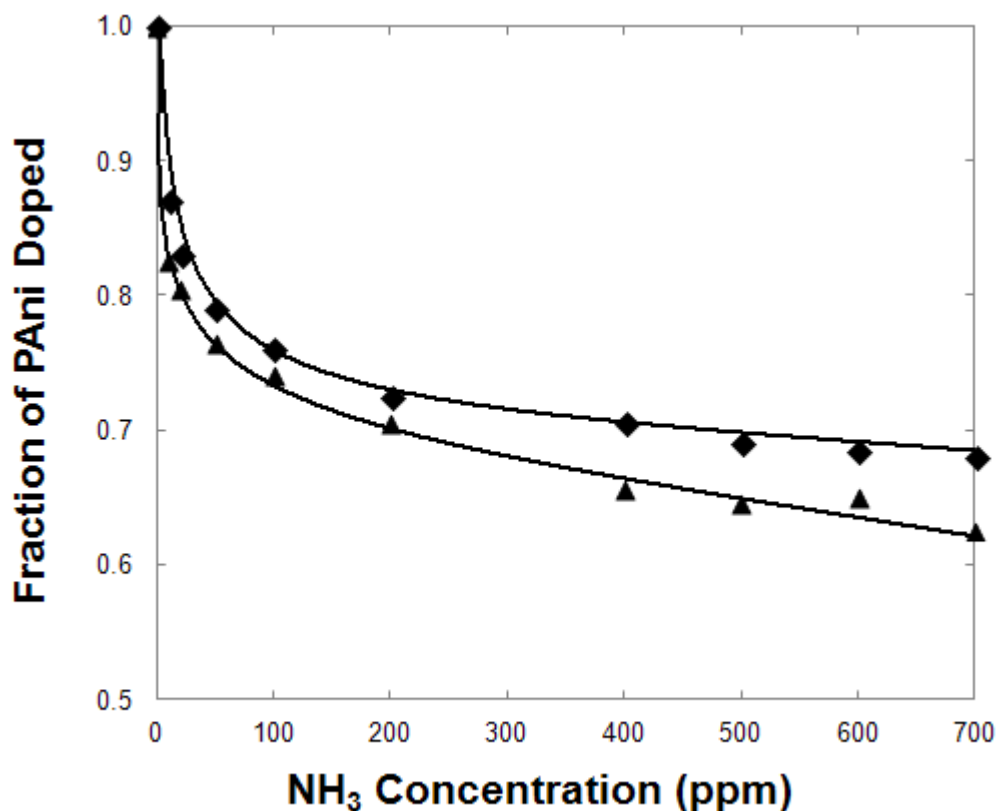
Figure 9 Equilibrium fraction of PAni doped (after partial de-doping by the gas) in the fibers derived from sensing responses at different ammonia concentrations. As-spun fibers (d = 620 nm) (filled diamonds); solid-state drawn fibers (d = 450 nm) (filled triangles).

For each data point in Figure 9, the fraction of PAni doped corresponds to a value of $K[NH_3]_s/[NH_4^+]_s$ according to Equation 9. Here, the subscript s is used to emphasize that these are concentrations of the ammonia and ammonium ion in the solid phase of the fiber, rather than the gas phase. The concentration of ammonia at the surface of the fiber is assumed to be in equilibrium with the exposed gas phase concentration of ammonia, with a partition coefficient, S, $[NH_3]_s = S[NH_3]_g$ according to Henry's Law. At steady state, this same concentration of ammonia pervades the entire fiber. The concentrations of de-doped PAni and ammonium ion are

both equal to the extent of reaction, ξ, as neither was present in the fiber initially, and neither species diffuses within the fiber. This allows the equilibrium constant K to be expressed in terms of the extent of reaction as follows

$$K = \frac{[NH_4^+]_s [PAni]}{[NH_3]_s [PAni-H^+]} = \frac{\xi^2}{S[NH_3]_g \left([PAni]_o - \xi\right)} \tag{10}$$

which is a quadratic equation in ξ

$$\xi^2 + SK[NH_3]_g \xi - SK[NH_3]_g [PAni]_o = 0 \tag{11}$$

The non-negative root of the equation is thus

$$\xi = \frac{\sqrt{(SK)^2 [NH_3]_g^2 + 4SK[NH_3]_g [PAni]_o} - SK[NH_3]_g}{2} \tag{12}$$

The values of external ammonia concentrations are known. For the as-spun PAni fibers, $[PAni]_0 = 5.0 \times 10^3$ mol/m^3, based on the known fiber density value of 1.0 g/cm^3.[25] Assuming a value for SK, we solve for the theoretical extent of reaction corresponding to each gas concentration, and obtain theoretical values for $K[NH_3]_s/[NH_4^+]_s = \xi/([PAni]_0 - \xi)$ at each concentration. A least-squared residual analysis is then performed on the difference between experimental and theoretical values of $(K[NH_3]_s/[NH_4^+]_s)$ to find the value of SK that best fits the data.

From the experimental steady-state data for the ammonia sensing by as-spun fibers (620 nm in diameter), the value of the equilibrium constant SK was thus determined to be 1.5 ± 0.1. Using this value, the theoretical values are plotted in **Figure 10** as the solid curve.
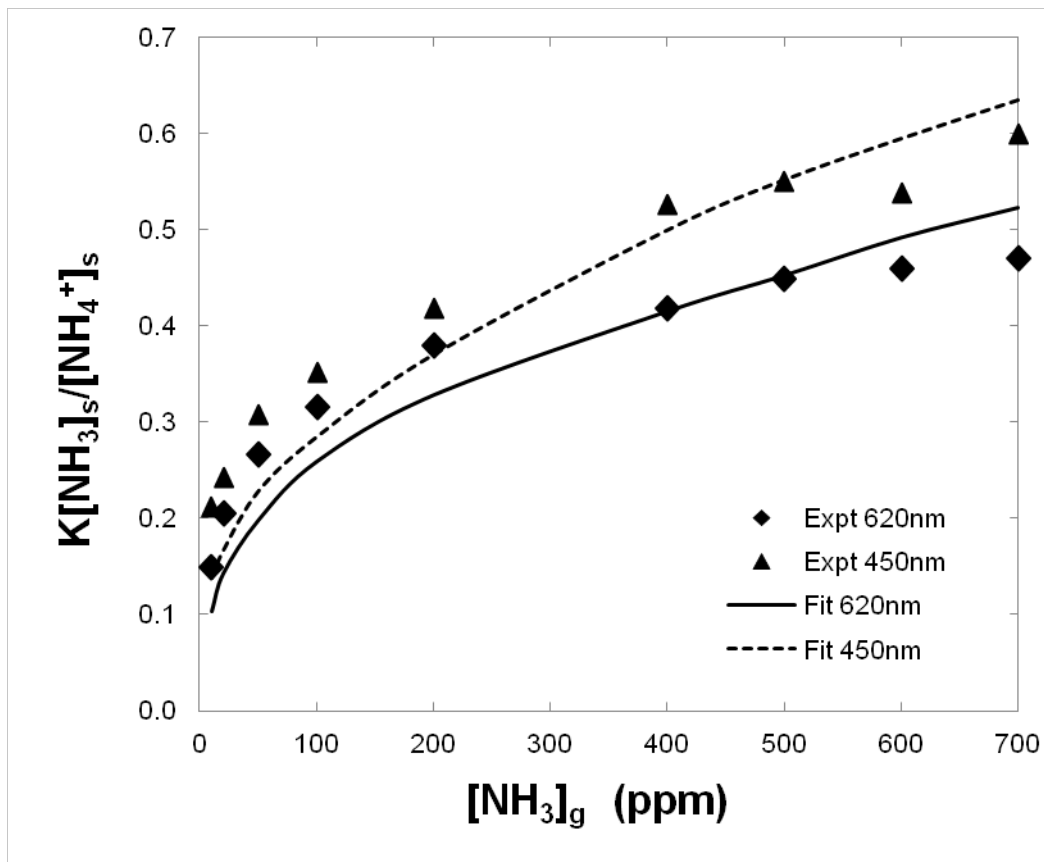

Figure 10 Comparison of experimental data (markers) and fitted values (solid and dotted lines) for both as-spun and solid-drawn doped PAni fibers upon ammonia exposure with concentrations ranging from 10 to 700 ppm

As can be seen from Figure 10, the experimental results for equilibrium extent of reaction for the 620 nm fibers and the 450 nm are systematically different over the whole range of external gas concentrations. We speculate that the solid state drawing process used to produce

the smaller diameter fibers results in small but significant changes in the morphology, which may be reflected by subtle changes in S and/or [PAni]$_0$. For purpose of the present analysis, we held constant the value of $SK = 1.5$ obtained for the as-spun fibers and varied [PAni]$_0$ in order to obtain the least squares residual for the data from the solid-state drawn fibers (450 nm diameter), The value obtained was [PAni]$_0 = 3.8 \times 10^3$ mol/m^3. The theoretical curve using these values is shown in Figure 10 as the dotted line.

In order to separate the estimate of SK into values for S and K, respectively, the results of the QCM analysis were used to determine the change in mass of the electrospun fiber sample (d = 620 nm) before and after exposure to various concentrations of NH$_3$ in nitrogen. Assuming that the change in mass is due entirely to uptake of ammonia, a portion of which is converted to ammonium ion, the change in mass can be expressed by Equation 13,

$$\frac{\Delta m}{m_o} = \frac{S[NH_3]_g + \xi}{[PAni]_o} \quad .$$

(13)

where m_0 is the original mass of the fibers obtained from the change in frequency due to deposition of fibers before exposure to gas, Δm is the change in mass calculated from frequency shifts due to gas exposure. From the expression for ξ in Equation 12, and known values of SK, gas concentrations and PAni concentrations, the value of S was determined at each of the three gas concentrations tested, and is shown in **Table 4**; the average gives $S = 0.05 \pm 0.01$. The value of the equilibrium constant is then determined to be $K = 30 \pm 8$.

Table 4 Calculation of Partition Coefficient, S, of ammonia in as-electrospun PAni fibers (d = 620nm)

31

$[NH_3]_g$ (ppm)	$\Delta m/m_0$	ξ (mol/m^3)	S
100	0.098 ± 0.002	500 ± 60	0.045 ± 0.005
500	0.206 ± 0.002	1100 ± 80	0.055 ± 0.005
700	0.239 ± 0.003	1200 ± 90	0.049 ± 0.008

Having determined values for S and K, henceforth for purposes of dynamical analysis, the reference concentration for Θ is the solid phase concentration of ammonia at the surface of the fiber ($r = 1$), which is related to the gas phase concentration of ammonia by the partition coefficient, S; that is, $C_{o,\Theta} = [NH_3]_{s,r=1} = S[NH_3]_g$ according to Henry's Law. Assuming that the reaction rate constants, diffusivity, and partition coefficient are not functions of gas concentration or fiber diameter, and that the gas phase is well mixed, the ratio $(k_f/D) = Da/S[NH_3]_g L^2$ is a parameter that can be determined by fitting to dynamical data such as that shown in Figure 4. The other variable in the model is $\tau = tD/L^2$, where real time t and fiber diameter L are known. We then fit the time-dependent sensing data with the modeled values to obtain estimates for k_f and D. Figure 12 shows the reaction-diffusion model results for $K = 30$ and $S = 0.05$. A least-squares residual fitting using all of the time-dependent data for as-spun fibers (620 nm diameter) measured with gaseous ammonia concentrations from 10 ppm to 500 ppm gives the diffusivity $D = (3.0 \pm 0.5) \times 10^{-11}$ cm^2/s, and the forward rate constant $k_f = 0.15 \pm 0.07$ cm^3/mol/s. The comparison between experimental gas sensing data and resistance change values fitted using the model is shown in **Figure 11**. These values are in reasonable agreement

with reported literature values, where the diffusion coefficient of ammonia in polymer is on the order of 10^{-11} to 10^{-9} cm^2/s,[26] and k_f is on the order of 0.001 to 0.1 cm^3/mol/s.[27, 28]
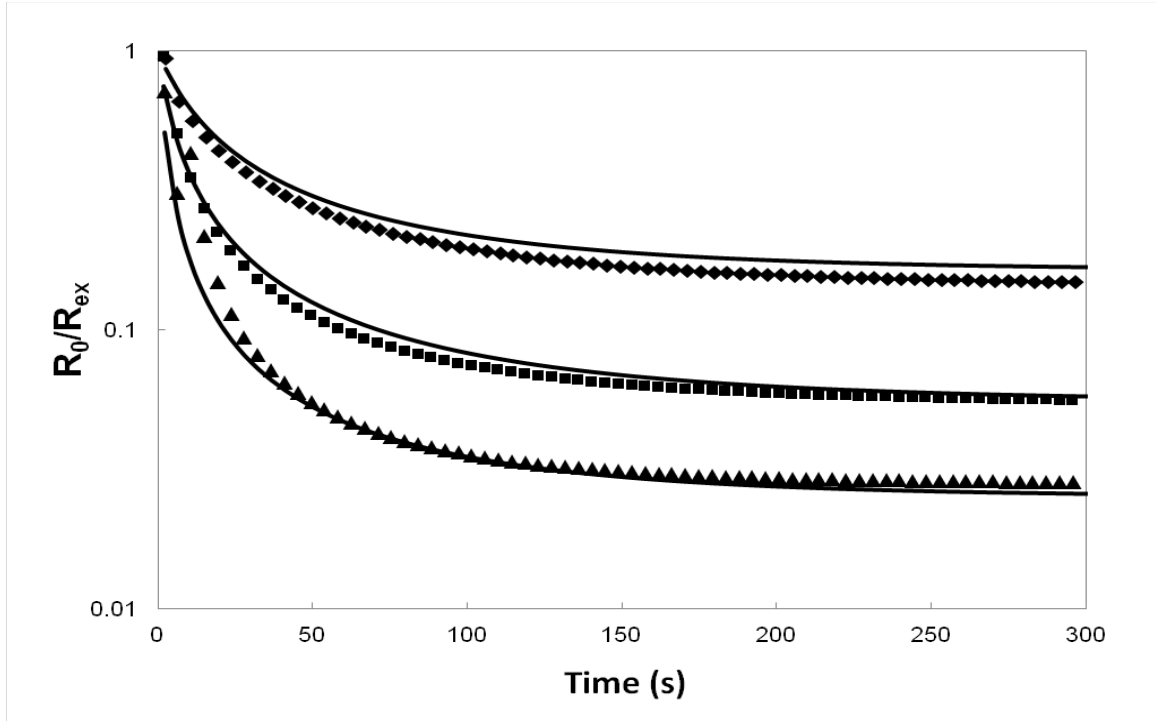

Figure 11 Comparison of experimental time-dependent gas sensing data (markers) and resistance change values fitted using the model (solid lines) for three sensing response time series: at external ammonia concentrations of 20 ppm (filled diamonds), 100 ppm (filled squares), and 500 ppm (filled triangles)

Table 5 Summary of Values for Fitted Model Parameters

Fitted Parameter	Value
SK	1.5 ± 0.1
S	0.05 ± 0.01
K	30 ± 8

33

|	
D	$(3.0 \pm 0.5) \times 10^{-11} \text{ cm}^2/\text{s}$
k_f	$0.15 \pm 0.07 \text{ cm}^3/(\text{mol s})$

3.6   Application of Model for Design Optimization

For optimization purposes, we assume that detection is required within a predetermined time, e.g., t = 60 s. For the 450 nm diameter PAni fibers at 500 ppm of ammonia exposure in air at a density of approximately 1 kg/m³, and the values provided in **Table 5**, we obtain τ = 3.6 and Da = 0.23. From the model plots in **Figure 12**, we find the optimal condition for this value of τ to be Da = 2.3 and R_0/R_{ex} = 0.0020. That is, for the 450 nm PAni fibers studied here, the optimal detection at 60 s corresponds to a $\Delta R/R_0$ of about 500, obtained under 5000 ppm of NH_3 exposure:

$$\left(\frac{\Delta R}{R_0}\right)_{opt,\tau=3.6} = \left[\left(\frac{R_0}{R_{ex}}\right)_{opt}\right]^{-1} - 1 = 500 \tag{14}$$

$$\frac{\text{Da}_{opt}}{\text{Da}_{ref}} = \frac{([NH_3]_g)_{opt}}{([NH_3]_g)_{ref}} \quad \Rightarrow \quad ([NH_3]_g)_{opt} = \frac{2.3}{0.23} \times 500\,ppm = 5000\,ppm \tag{15}$$

For the same detection time of t = 60 s and L = 620 nm, τ = 1.9 and the optimal values are Da = 5.5 and R_0/R_{ex} = 0.0025, corresponding to a $\Delta R/R_0$ ratio for PAni of this fiber diameter (620 nm) of 390 at 6200 ppm of NH_3 exposure.

34

Next, we optimize fiber diameter for a given detection time and gas exposure. In this case, both τ and Da vary with L, so the optimization trajectory does not follow a single contour line shown in Figure 12. Instead, the product, $\tau Da = t k_f S[NH_3]_g$ is constant. For a detection time of 60 s and exposure to a concentration of 500 ppm, the best sensing results are obtained at Da = 0.016 and $\tau = 52$, with $R_0/R_{ex} = 0.029$. This condition corresponds to a fiber diameter of 60 nm, and is expected to show a ratio of resistance change of $\Delta R/R_0 = 36$ after 60 s of exposure.
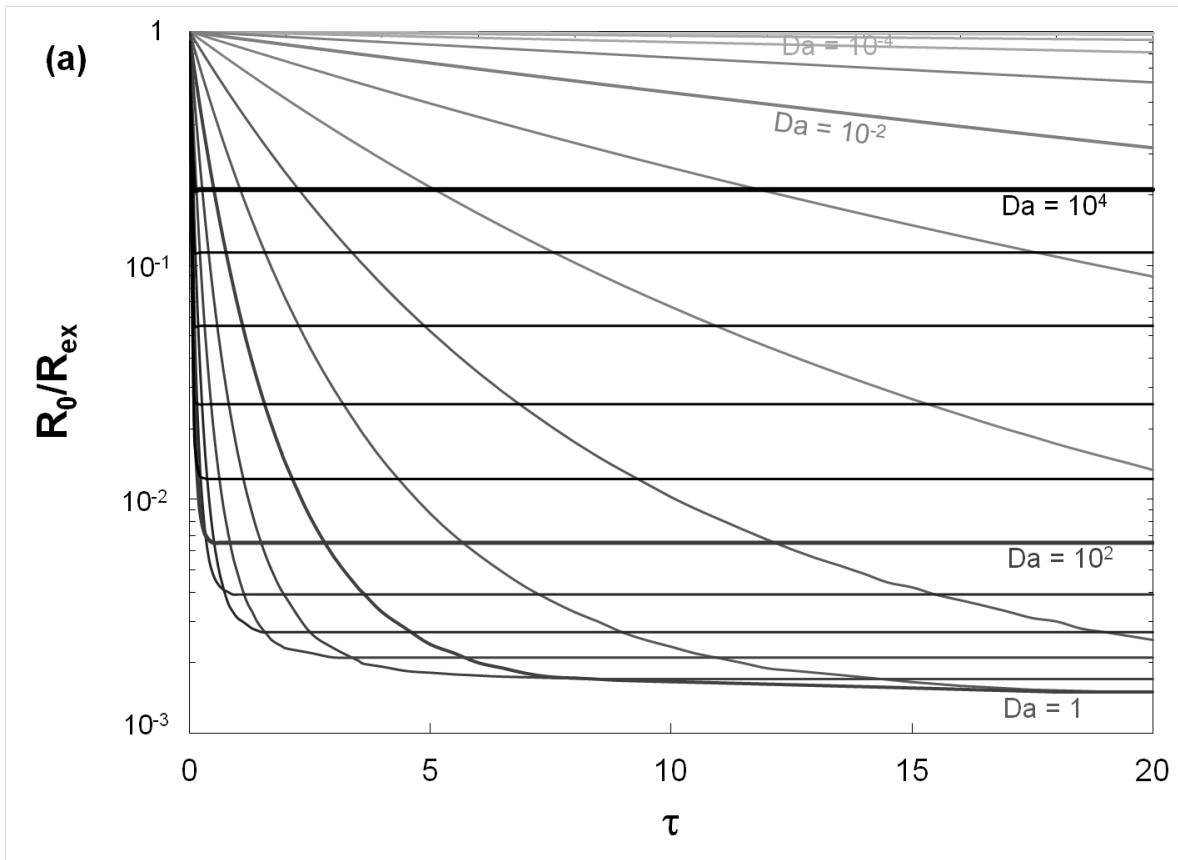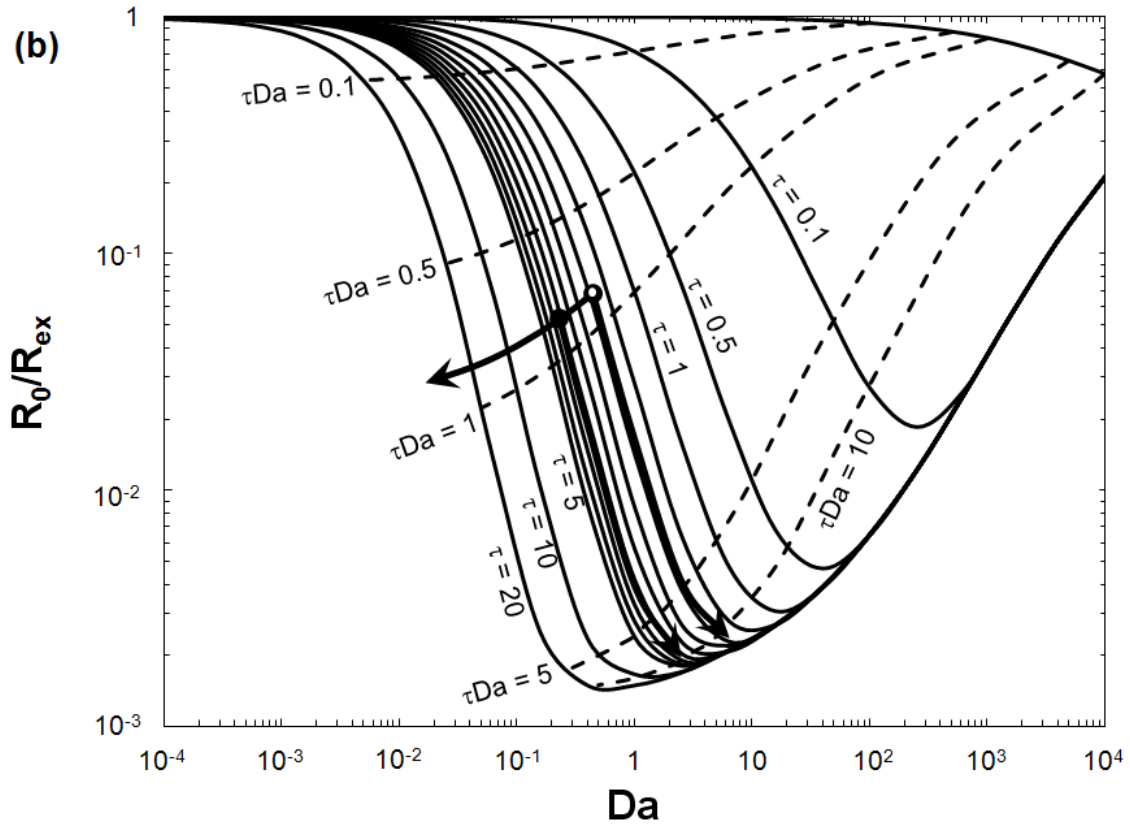
Figure 12 Reaction-diffusion model results at K = 30 using the experimental NH_3 sensing parameters shown in Table 5; (a) a plot of resistance ratio versus τ for Da ranging from 10^{-4} to 10^4 (log increment of 0.4); (b) a plot of resistance ratios versus Da for τ ranging from 0 to 20 (increment of 0.5 between $\tau = 1$ and $\tau = 5$); dotted lines show the contours with constant τDa values; the open and filled circles indicate the locations of the 620 nm fiber and 450 nm fiber at t = 60 s respectively, and the arrows indicate the optimization trajectories for the examples discussed in the text.

4.   Conclusions

Pure PAni fibers with different levels of doping and good molecular alignment have been fabricated by coaxial electrospinning and subsequent removal of the shell by dissolution. These fibers are found to be very effective nanoscale sensors for ammonia and nitrogen dioxide gases, both toxic gases harmful to humans and the environment even when exposed in concentrations as low as tens of ppm. Both sensitivity and response times are shown to be excellent, with response ratios up to almost 60-fold for doped PAni sensing of NH_3 up to 700 ppm, and more than five orders of magnitude for NO_2 sensing by undoped PAni fibers at concentrations as low as 50 ppm. The characteristic times for the gas sensing are shown to be on the order of 1 to 2 minutes. Both gases are found in a variety of industrial environments; the simple yet fast and sensitive detection demonstrated by these PAni fibers can be very useful in industrial leak detection or similar situations. To the best of our knowledge, the five orders of magnitude change in resistance in response to 50 ppm of NO_2 gas exposure at room temperature is the largest reported to date, including conducting polymer sensors, metal-oxide sensors and catalytic detectors, and gives rise to excellent signal clarity and low detection threshold. For the purpose of detailed investigation of gas sensing in nanofibers in general, we also present a generic time-dependent reaction-diffusion model that accounts for reaction kinetics, reaction equilibrium, and diffusivity parameters. The model allows for the extraction of key parameters from experimental data, and can be used to predict and optimize the fibers for gas sensing under different conditions.

5.   Acknowledgements

[1]   X.Y. Wang, C. Drew, S.H. Lee, K.J. Senecal, J. Kumar, L.A. Sarnuelson, *Nano Lett.* **2002,** *2*, 1273-1275

[2]   I. Kim, A. Rothschild, B.H. Lee, D.Y. Kim, S.M. Jo, H.L. Tuller, *Nano Lett*. **2006**, *6*, 2009-2013

[3]   C.N. Hoth, S.A. Choulis, P. Schilinsky, C.J. Brabec, *Adv. Mater*. **2007,** *19*, 3973-3978

[4]   A. Kolmakov, Y. Zhang, G. Cheng, M. Moskovits, *Adv. Mater.* **2003**, *15*, 997-1000

[5]   S. Ji, X. Wang, C. Liu, H. Wang, T. Wang, D. Yan, *Organic Electronics* **2013**, *14*, 821-826

[6]   S.H. Choi, S.J. Choi, B.K. Min, W.Y. Lee, J.S. Park, I. Kim, *Macromol. Mater. Eng.* **2013**, *298*, 521-527

[7]   N.J. Pinto, D. Rivera, A. Melendez, I. Ramos, J.H. Lim, A.T. Johnson, *Sensors & Actuators B* **2011**, *156*, 849-853

[8]   D. Bhattacharyya, K. Senecal, P. Marek, A. Senecal, K.K. Gleason, *Adv. Funct. Mater.* **2011**, *21*, 4328-4337

[9]   N. Liu, G. Fang, J. Wan, H. Zhou, H. Long, X. Zhao, *J. Mater. Chem.* **2011**, *21*, 18962-18966

[10]   Y.M. Shin, M.M. Hohman, M.P. Brenner, G.C. Rutledge, *Appl. Phys. Lett.* **2001**, *78*, 1149-1151

[11]   H.D. Tran, D. Li, R.B. Kaner, *Adv. Mater.* **2009**, *21*, 1487-1499

[12]   J.H. Yu, S.V. Fridrikh, G.C. Rutledge, *Polymer* **2006,** *47*, 4789-4797

[13]   Y. Zhang, G.C. Rutledge, *Macromolecules* **2012**, *45*(10), 4238-4246

[14]   B. Ding, M. Wang, J. Yu, G. Sun, *Sensors* **2009**, *9*, 1609-1624

[15]   Z.C. Sun, E. Zussman, A.L. Yarin, J.H. Wendroff, A. Greiner, *Adv. Mater.* **2003,** *15*, 1929-1932

[16]   J.H. Yu, S.V. Fridrikh, G.C. Rutledge, *Adv. Mater.* **2004,** *16*, 1562-1566

[17]   D.P. Volanti, A.A. Felix, M.O. Orlandi, G. Whitfield, D.J. Yang, E. Longo, H.L. Tuller, J.A. Varela, *Adv. Funct. Mater.* **2013**, *23*, 1759-1766

[18]   F. Hook, M. Rodahl, P. Brzezinski, B. Kasemo, *Langmuir* **1998**, *14*, 729-734

[19]   M. Alf, T.A. Hatton, K.K. Gleason, *Langmuir* **2011**, *27*, 10691-10698

[20]   G. Sauerbrey, *Z. Physik* **1959**, *155*, 206-222

[21]   J. Stejskal, I. Sapurina, M. Trchová, J. Prokes, I. Krivka, E. Tobolková, *Macromolecules* **1998,** *31*, 2218–2222

[22]   Z. Wu, X. Chen, S. Zhu, Z. Zhou, Y. Yao, W. Quan, B. Liu, *Sensors & Actuators B* **2013**, *178*, 485-493

[23]   S. Christie, E. Scorsone, K. Persaud, F. Kvasnik, *Sensors & Actuators B* **2002**, *90*, 163-169

[24]   The U.S. Environmental Protection Agency: National Ambient Air Quality Standards (NAAQS), http://www.epa.gov/air/criteria.html, accessed: May, 2013

[25]   T.A. Skotheim, R.L. Elsenbaumer, J.R. Reynolds, Eds., in *Handbook of Conducting Polymers*; Marcel Dekker: New York, NY, USA **1998**

[26]   H. Liu, J. Kameoka, D.A. Czaplewski, H.G. Craighead, *Nano Lett.* **2004**, *4*, 671-675

[27]   Q. Lin, Y. Li, M. Yang, *Sensors & Actuators B* **2012**, *161*, 976-982

[28]   S. Kuwabata, C.R. Martin, *J. Membr. Sci.* **1994**, *91*, 1-12

ToC Entry

   Electrospun polyaniline fibers have been fabricated and evaluated as chemiresistive gas sensors. The fibers exhibit remarkable changes in measured resistances for ammonia and nitrogen dioxide sensing, with short characteristic response times. A time-dependent reaction-diffusion model is used to extract physical parameters from fitting experimental data, and to illustrate the selection of optimal material design parameters for gas sensing by nanofibers.

ToC Figure